Nohmi, T., et al. Basic Research On Condensed Matter Nuclear Reaction Using Pd Powders Charged With High Density Deuterium. in ICCF-14 International Conference on Condensed Matter Nuclear Science. 2008. Washington, DC.

Basic research on condensed matter nuclear reaction using Pd powders charged with high density deuterium

T. Nohmi[1], Y. Sasaki[1], T. Yamaguchi[1], A. Taniike[1], A. Kitamura[1], A. Takahashi[2], R. Seto[2], Y. Fujita[2]

[1] *Division of Marine Engineering, Graduate School of Maritime Sciences, Kobe University*
5-1-1 Fukaeminami-machi, Higashinada-ku, Kobe 6580022, Japan
[2] *Technova Inc.*
The Imperial Hotel Tower, 13F, 1-1 Uchisaiwaicho 1-chome, Chiyoda-ku, Tokyo 1000011, Japan

Abstract

We have constructed an experimental system to replicate the phenomenon of heat and ^{4}He generation by D_2 gas absorption in nano-sized Pd powders reported by Arata, [1] and to investigate the underlying physics. We performed calorimetry during D_2 or H_2 absorption with micronized powders of Si, Pd and Pd-black. With Pd-black and D_2, after the palladium deuteride formed, the cell produced 8.3 ±4.5 kJ (or 2.6 ±1.4 kJ/g), which is somewhat larger than the systematic error of 4.0 kJ estimated from a D_2 blank.

1. Introduction

Arata recently reported [1] that high purity D_2 gas charging of Pd nano-powders in the form of Pd/ZrO_2 nano-composite induced significantly higher temperatures inside the reactor vessel than on the outside wall, while blank runs using H_2 gas showed almost no temperature difference. The temperature difference lasted for more than 50 hours. To verify that the excess heat came from a nuclear reaction, QMAS was employed to show the existence of ^{4}He as nuclear ash in the vessel. The phenomenon seemed to be highly reproducible as long as the same test equipment was used.

In the present work we constructed an experimental system to replicate the phenomenon of heat and ^{4}He generation and to investigate the underlying physics. We report preliminary results.

2. D_2/H_2 absorption system

The system is composed of two identical chambers (a twin system): one for a D_2 gas foreground run, and the other for H_2 gas blank run. Each system has an inner reaction chamber containing Pd powder and an outer chamber that is evacuated to provide thermal insulation. Inside the reaction chamber is located a sample cup, around which a heater is wound for baking. In addition to thermocouples located on the sample cup and the outer surface of the reaction chamber for temperature measurement, a pair of thermocouples is provided for flow calorimetry to estimate the heat production rate by measuring the temperature difference between the inlet and the outlet of a cooling water pipe. The D_2 gas is nominally 99.5% pure and the H_2 is 99.998% pure. Flow rate control of D_2/H_2 gas purified with a liquid-nitrogen cold trap is made with a Pd membrane filter which also serves as an additional purifier.

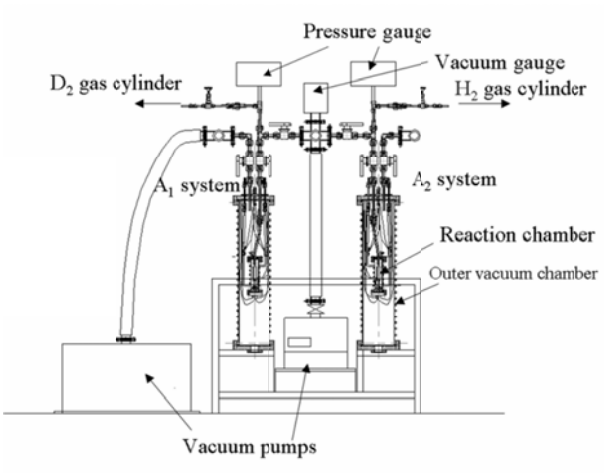

Figure 1. Simplified view of the system

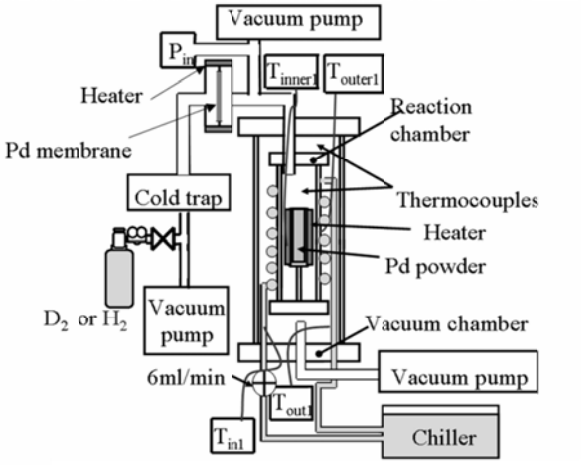

Figure 2. Functional view of the system

The reaction chamber is thermally isolated by evacuating the outer vacuum chamber. We measured the heat recovery rate with flow calorimetry under a variety of conditions: with input power of 1 W, 3 W, 6 W and 10 W; and reaction chamber D_2 gas pressure of 0 MPa, 0.1 MPa, 0.3 MPa and 1.0 MPa. The coolant flow rate was 6 ml/min in all cases.

We observed a temperature variation after changing the input power. Figure 3 shows the temperature difference during the power change from 10 W to 6 W. The variation is expressed by a sum of two exponential functions; one (0 ~ 700 s) with a time constant of τ_1, and the other (700 s ~) with τ_2. The values of τ_1 and τ_2 obtained from the fitting are listed in Table 1. The former we consider to be determined mainly by heat transfer from the cup to the reaction chamber due to convection and conduction through D_2/H_2 gas, while the latter is determined by conduction losses from the reaction chamber to the outer chamber.

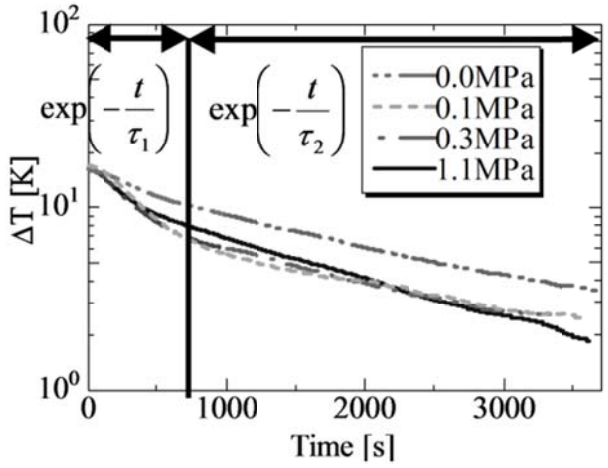

Figure 3. Calibration of flow calorimetry

Table 1. Thermal time constant deduced from the decay curves in Fig. 3.

MPa	τ_1 [s]	τ_2 [s]
0	1500	2700
0.1	690	3000
0.3	750	2600
1	930	2000

The heat recovery rate is summarized in Table 2. It is 66% ± 7%; and it is only marginally dependent on pressure and the input power.

Table 2. Heat recovery rate.

Pressure[MPa]	Input power [W]	Output power [W]	Heat recovery rate
0	10.0	5.9	59.3%
0	6.1	4.1	68.2%
0	3.0	2.2	72.5%
0	1.0	0.7	67.5%
3	10.0	7.0	70.2%
3	6.1	4.3	69.7%
3	3.0	2.2	71.8%
3	1.0	0.5	51.9%
1	10.0	6.8	68.1%
1	6.1	4.3	70.7%
1	3.0	2.0	68.3%
1	1.1	0.6	53.4%

4. Performance test of the Pd membrane filter

The Pd membrane (0.2 mm-t, 99.95%) separates the evacuated reaction chamber (1.6 ℓ) and the gas reservoir filled with D_2 at 1 MPa. The permeation rate of D_2 gas into the reaction chamber was derived as a function of membrane temperature by measuring the rate of pressure increase after stopping evacuation. Results are shown in Fig. 4. The D_2 gas flow rate is shown to be controllable between 0.1 and 25 sccm by varying the temperature from the room temperature to 900 K for membrane 2.

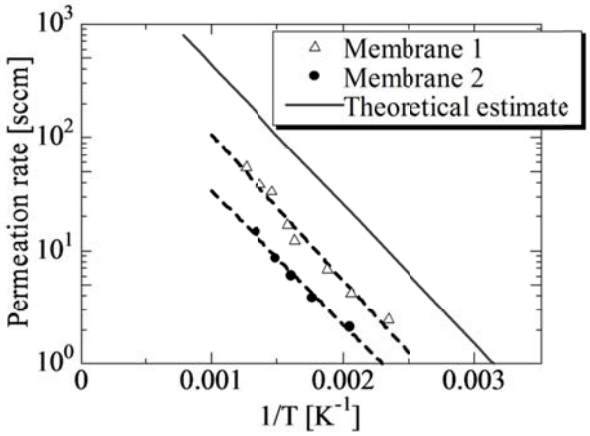

Figure 4. Permeation characteristics of the Pd membrane filter.

5. Blank run using a Si powder

We examined the temperature drift, or uncertainty, in the measurement of temperature using an 8-g, 150-mesh powder of Si with a purity of 99.999%. After evacuating the reaction chamber, the Si powder was baked at 470 K to outgas the Si powder. Next, highly pure D_2 gas was introduced into the reaction chamber through the Pd membrane filter. Figure 5 shows the variation of pressure in the system after introducing the D_2 gas, the inlet-outlet temperature difference ΔT of the coolant water, and the output power calculated from ΔT.

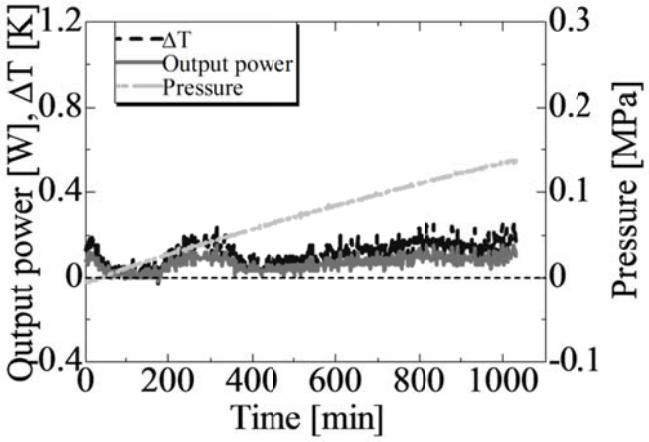

Figure 5. Evolution of temperature, heat and pressure in the vessel after exposure of the 150 mesh Si powder to D2 gas.

The D_2 pressure in the system rises immediately after D_2 gas is introduced. The rate of pressure rise indicates a gas flow rate of 0.27 sccm. The observed variations in the temperature; *i.e.*, a short-term oscillation (with a period of few minutes) of about 0.1 K and a long-term drift (over a few hours) of about 0.2 K, should be considered inherent in the measurement system, and taken into account also in the foreground runs with Pd powders. The error in energy due to the temperature drift amounts to 4.0 kJ for the 1000-minute run. This value is considered the error bound in output heat for the foreground runs in Tables 3 through 6.

6. 0.1-μm-diam. Pd powders with a purity of 99.5%

The sample cup was filled with 5 g of Pd powder with particle diameter size of 0.1 μm and a purity of 99.5%. The reaction chamber was evacuated, and the Pd powder was baked at 430 K. Then high purity D_2 or H_2 gas was introduced into the reaction chamber through the Pd membrane filter. The results are shown in Fig. 6 and 7 for two cases of D_2 absorption, and in Fig. 8 for H_2 absorption.

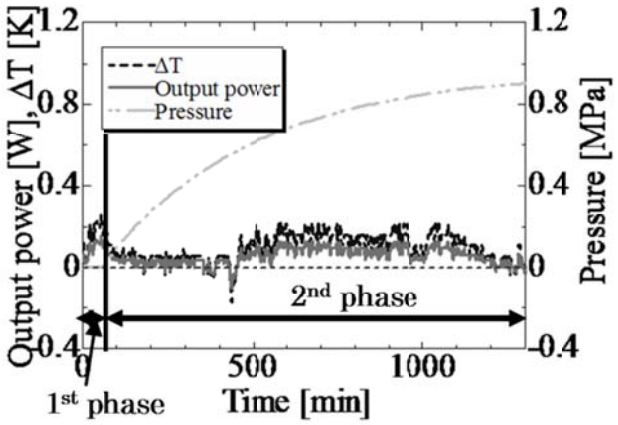

Figure 6. Absorption run for the 0.1-μm-diam. Pd powder. The D2 gas flux is 4.3 sccm.

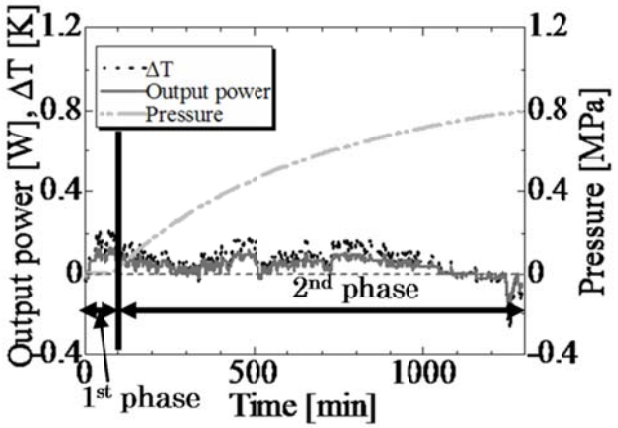

Figure 7. Absorption run for the 0.1-μm-diam. Pd powder. The D2 gas flux is 3.5 sccm.

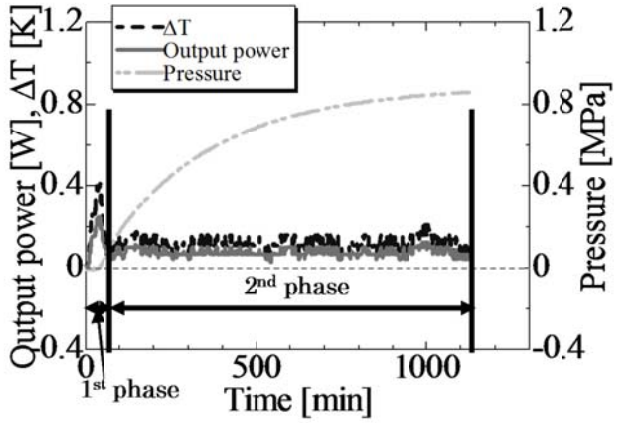

Figure 8. Absorption run for the 0.1-μm-diam. Pd powder. The H_2 gas flow rate is 6.8 sccm.

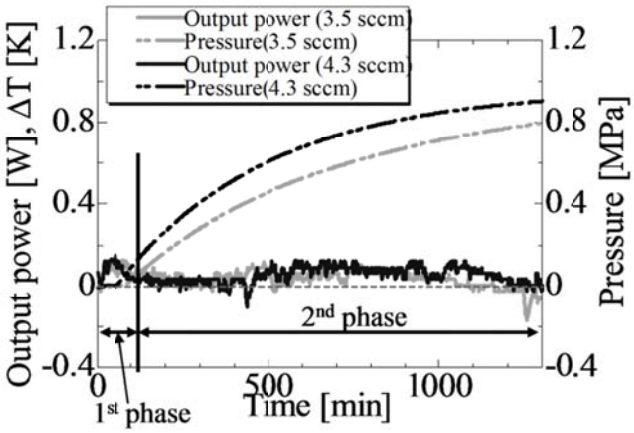

Figure 9. Absorption run for the 0.1-μm-diam. Pd powder; effect of flow rate.

After the gas is introduced, pressure does not begin to rise for a while. During this 1st phase the Pd powder absorbs almost all of the D_2 or H_2 gas as it flows in, and heat is released from the formation of the deuteride or hydride. Loading is estimated to reach $PdD_{0.43}$ or $PdH_{0.45}$. After about 30 minutes, the powder seems to stop absorbing gas; gas pressure begins to rise; and the heat release from deuteride or hydride formation subsides.

The performance with H_2 and D_2 gas was compared. The output energy in the 1st phase with H_2 (Fig. 8) is almost the same as that of D_2, and is consistent with the nominal value of 100 to 405 J/g for the heat of hydride formation. The output energy in the 2nd phase appears to be larger for H_2 than D_2. However, the difference is smaller than the error mentioned above, and is not meaningful in this case.

7. 300-mesh, 99.9% pure Pd black

The performance of Pd black absorption of D_2 (flow rate 4.5 sccm) was compared with H_2 (flow rate 5.6 sccm). Results are shown in Fig. 10 and summarized in Table 5. Much higher loading to $PdD_{0.85}$ or $PdH_{0.78}$ is realized compared to that in the case of 0.1-μm-diam. Pd powder. The output energy in the 1st phase is almost the same for D_2 and H_2. It seems to be somewhat larger than the nominal values of 80 - 330 J/g (D_2) and 100 - 405 J/g (H_2). On the other hand, the output energy of 8.3 ± 4.5 kJ and 2.6 ± 1.4 kJ/g in the 2nd phase of D_2 absorption appears to be larger than that in the case of H_2. The difference is appreciably greater than the error due to the temperature drift of 5.5 kJ mentioned above for the Si blank run.

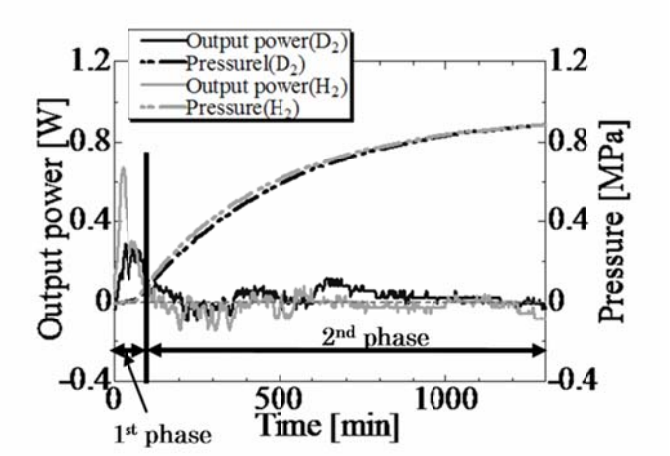

Figure 10. Absorption runs for 300-mesh Pd black; effect of gas species.

Table 3. Integrated output power for the 0.1-μm-diam. Pd powder; effect of flow rate.

	3.5 sccm	4.3 sccm
1st phase	$(1.0\pm0.7)\times10^2$ J/g	$(1.0\pm0.5)\times10^2$ J/g
2nd phase	$(5.2\pm8.3)\times10^2$ J/g	$(7.9\pm8.8)\times10^2$ J/g

Table 4. Integrated output power for the 0.1-μm-diam. Pd powder; effect gas species

	D_2	H_2
1st phase	$(1.0\pm0.5)\times10^2$ J/g	$(1.2\pm0.3)\times10^2$ J/g
2nd phase	$(7.9\pm8.8)\times10^2$ J/g	$(1.1\pm0.8)\times10^3$ J/g

Table 5. Results of absorption runs for 300-mesh Pd black; effect of gas species

	D_2	H_2
1st phase	$(5.4\pm1.0)\times10^2$ J/g	$(4.5\pm0.8)\times10^2$ J/g
2nd phase	$(2.6\pm1.4)\times10^3$ J/g	$(-6.2\pm13)\times10^2$ J/g

Table 6. Summary of the results of absorption runs.

Sample	weight [g]	Gas	Nominal flow rate [sccm]	Measured flow rate [sccm]	1st phase [J]	2nd phase [J]	1st phase [J/g]	2nd phase [J/g]	D/Pd or H/Pd
0.1μϕ–Pd	5	D_2	10	3.5	$(5.1\pm3.5)\times10^2$	$(2.5\pm4.1)\times10^3$	$(1.0\pm0.7)\times10^2$	$(5.2\pm8.3)\times10^2$	0.46
0.1μϕ-Pd	5	D_2	25	4.3	$(4.8\pm2.4)\times10^2$	$(4.0\pm4.4)\times10^3$	$(1.0\pm0.5)\times10^2$	$(7.9\pm8.8)\times10^2$	0.43
0.1μϕ-Pd	5	H_2	25	6.8	$(5.8\pm1.7)\times10^2$	$(5.6\pm3.9)\times10^3$	$(1.2\pm0.3)\times10^2$	$(1.1\pm0.8)\times10^3$	0.45
Pd black	3.2	D_2	25	4.5	$(1.7\pm0.3)\times10^3$	**$(8.3\pm4.5)\times10^3$**	$(5.4\pm1.0)\times10^2$	**$(2.6\pm1.4)\times10^3$**	**0.85**
Pd black	3.6	H_2	25	5.6	$(1.6\pm0.3)\times10^3$	$(-2.2\pm4.6)\times10^3$	$(4.5\pm0.8)\times10^2$	$(-6.2\pm13)\times10^2$	**0.78**

8. Concluding remarks

A Pd-H_2 / D_2 gas absorption system using commercial Pd powders has been constructed, with flow calorimetry and nuclear diagnosis. Calibration of the system and preliminary experimental results have been described. The results of the present work are summarized in Table 6.

When D_2 gas was used with Pd-black, apparent excess heat production was observed. However, temperature oscillations and drift were relatively large, so the accuracy of the system must be improved to confirm the result. For example, the time constant of the calorimeter has to be decreased by decreasing the heat capacity of the reaction chamber. Increasing the mass of the test sample should also help obtain clearer heat evolution. Nano-sized powders of Pd as well as a variety of alloy powders also deserve examination.

Reference

1. Y. Arata, et al.; The special report on research project for creation of new energy, J. High Temperature Society, No. 1. 2008.